International Journal of Engineering Research & Technology (IJERT)
ISSN: 2278-0181
Vol. 15 Issue 05 , May - 2026

Effect of Nanoparticle-Doped Activated Flux on Weld Penetration and Microstructure in MIG Welding of AISI 1018 Steel

Mr S Abishek
PG Scholar
Department of Engineering Design
Government College of Technology
Coimbatore, India

Mr S Bradeesh moorthy
Assistant Professor
Department of Mechanical Engineering
Government College of Technology
Coimbatore, India

***Abstract* - This study investigated the influence of a specially formulated nanoparticle-doped activated flux on the MIG welding performance of AISI 1018 mild steel. The flux mixture, consisting of TiO_2 nanoparticles, borax, and extracted electrode flux blended with an acetone–isopropanol solvent, significantly enhanced the welding characteristics. The microstructural analysis showed that the flux-coated weld exhibited finer and more compact dendritic grains due to improved arc constriction and controlled heat flow. Macrostructural observations confirmed deeper penetration and a sharper fusion boundary, indicating effective modification of molten metal flow. The hardness distribution across the weldment displayed higher and more consistent values in the flux-coated sample, reflecting refined microstructure and efficient thermal regulation. The tensile test further validated the weld strength, demonstrating that the flux-coated joint possessed adequate load-bearing capacity and uniform deformation behavior. Overall, the results confirm that the activated flux contributed to improved weld quality, enhanced penetration, and better mechanical performance compared to conventional MIG welding without flux.**

Keywords* - *MIG welding, Activated flux, TiO_2 nanoparticles, AISI 1018 mild steel, Weld penetration, Microstructural analysis, Mechanical properties, Nanoparticle-doped flux.

I. INTRODUCTION

Welding is one of the most essential fabrication processes in modern manufacturing industries. It provides a permanent joint between metallic parts through localized coalescence achieved by the application of heat and, in some cases, pressure. Among the several welding processes available, Metal Inert Gas (MIG) welding, also known as Gas Metal Arc Welding (GMAW), is widely used due to its high deposition rate, ease of automation, and ability to weld ferrous and non-ferrous materials. However, a major limitation of conventional MIG welding is shallow weld penetration, which restricts its effectiveness for thicker sections. To overcome this limitation, recent research has focused on Activated Flux MIG (A-MIG) or Activated TIG (A-TIG) welding techniques, where a thin coating of specially formulated flux is applied to the surface prior to welding. The flux modifies the heat and fluid flow within the weld pool, improving penetration and overall weld quality [1]. The manual GMAW (Gas Metal Arc Welding) setup was selected to provide greater control and flexibility over the welding parameters such as current, voltage, wire feed rate, and torch angle. This setup allowed the operator to adjust conditions in real time during welding, ensuring consistent bead formation and avoiding potential defects [2 - 4].

The performance of an activated flux depends primarily on its chemical composition and solvent base, which determine the nature of arc constriction, Marangoni convection, and the stability of the weld pool. The use of nanoparticles such as Titanium Dioxide (TiO_2) has been shown to enhance arc concentration and improve weld depth-to-width ratio (D/W). Similarly, borax-based fluxes help stabilize the arc and remove oxides from the weld surface, This study investigates a hybrid flux system composed of Borax, Extracted Flux (from electrode coating), and TiO_2 nanoparticles, dissolved in a solvent mixture of acetone and isopropanol (60:40 ratio). The combination aims to produce a more refined and concentrated arc column, improve weld pool fluidity, and yield a higher Penetration profile in MIG welding of AISI 1018 mild steel [5].

Although several advanced techniques have been proposed for welding defect identification and prediction, including machine vision–based inspection systems and artificial intelligence models, the primary focus of many of these studies has been on defect detection rather than defect formation mechanisms. For instance a machine vision system combined with neural networks to classify surface defects in MIG welded joints [6], and employed fuzzy logic modeling to predict weld bead penetration in submerged arc welding using process parameters and nanoparticle thickness [7]. Additionally, recent reviews have highlighted the operational characteristics and industrial relevance of TIG and MIG welding processes [8]. In contrast, the present study concentrates on analyzing how welding defects originate and develop under varying process conditions, providing insight into the metallurgical and process-related factors responsible for defect formation rather than automated defect identification.

Previous studies have shown that weld quality is highly influenced by modifications in welding conditions and consumables. The changes in shielding gas composition significantly affect fusion characteristics, microstructure, and mechanical properties in MIG-welded stainless steels [9].

International Journal of Engineering Research & Technology (IJERT)
ISSN: 2278-0181
Vol. 15 Issue 05 , May - 2026

Similarly, the use of active fluxes such as SiO_2 and MnO_2 enhanced weld penetration and microstructural refinement in TIG-welded low-carbon steel [10]. However, limited research exists on the application of nanoparticle-doped fluxes in MIG welding, particularly for AISI 1018 steel, which forms the focus of the present study.

The weld penetration and microstructural evolution are strongly influenced by weld pool dynamics, heat input, and flux-assisted modifications. Activated flux techniques have been shown to enhance penetration and depth-to-width ratio by altering arc behavior and Marangoni convection [11]. Investigations on dissimilar and high-energy welds further highlight that microstructure formation, strain localization, and joint integrity are governed by fusion zone characteristics and heat-affected zone control [12 & 13]. These findings emphasize the importance of flux-assisted process control for improving weld quality.

II. EXPERIMENTAL PROCEDURE

The procedures were carefully designed to study the effect of nanoparticle-doped activated flux on weld geometry, microstructure, and mechanical properties of AISI 1018 mild steel joints using the Metal Inert Gas (MIG) welding process. The experimental work was carried out in multiple stages, starting from material preparation, formulation of activated flux, setup of the welding system, parameter selection, and finally testing and evaluation of the welded samples. The intention behind this experimental design was to establish a correlation between process parameters, flux composition, and the resultant weld quality.

The base material selected for this investigation was AISI 1018 mild steel, chosen for its excellent weldability, good ductility, and uniform mechanical properties. The chemical composition of the base metal is shown in Table 1. The use of ER70S-6 filler wire, rich in silicon and manganese, ensures proper deoxidation during welding and enhances bead smoothness. The activated flux used in this research was prepared as a slurry by combining borax, titanium dioxide (TiO_2) nanoparticles, and flux extracted from the coating of E6013/E7018 electrodes. These powders were mixed with a 60:40 acetone–isopropanol solvent system, forming a uniform, easily applicable paste. The solvent system provides a homogeneous medium for dispersion of solid particles and controls the viscosity of the flux slurry. Acetone, being a fast-evaporating solvent, allows for rapid drying of the flux coating before welding, while isopropanol slows down evaporation slightly to promote even film formation and strong adhesion to the metal surface. The Composition of Flux Slurry is shown in Table 2.

The coating from E6013 electrodes was carefully removed using a scraper, crushed into a fine powder, to achieve uniform particle size. The extracted flux, TiO_2, and borax powders were oven-dried at 110°C for one hour to eliminate moisture, ensuring proper adhesion and preventing porosity during welding. Before welding, the surface of each work piece was cleaned using emery paper and acetone to remove any oxides or contaminants. The prepared flux slurry was applied uniformly along the weld line using a fine brush, maintaining a thickness of approximately 0.15–0.20 mm. The coated specimens were then allowed to dry naturally for 5–10 minutes until the solvent fully evaporated, forming a thin, stable coating suitable for welding.

The MIG welding equipment used operates on a constant voltage power source and is capable of delivering a maximum current of 250 A and an open-circuit voltage of 30 V. The process employs a continuous solid filler wire (ER70S-6, 1.2 mm diameter) fed through the torch, which melts under an electric arc formed between the consumable electrode and the work piece. The arc heat melts both the filler wire and the base metal, forming a molten pool that solidifies into the weld bead. The process parameters are mentioned in Table 3.

After welding, the specimens were sectioned perpendicular to the weld bead to prepare samples for metallurgical and mechanical characterization. The cross-sections were subjected to microstructural and microstructural examination to evaluate weld penetration, bead geometry, fusion zone, and heat-affected zone characteristics. Microstructural analysis was carried out on polished and etched samples using optical microscopy. Vickers micro hardness testing was performed across the weld metal, heat-affected zone, and base metal to assess hardness variation. Additionally, tensile tests were conducted on welded specimens to evaluate the mechanical performance.

TABLE I Chemical composition of AISI 1018 by weight %

Element	Composition
C	≤0.12
Mn	1.40–1.85
Si	0.80–1.15
P	≤0.025
S	≤0.035
Cu	≤0.50
Fe	Rest

TABLE II Composition of Flux Slurry by weight %

Component type	Material	Percentage by weight (%)
Base liquid	Acetone	60
	Isopropanol	40
Flux	Extracted Electrode Flux (E6013)	70
	Titanium Dioxide (TiO_2)	20
	Borax ($Na_2B_4O_7 \cdot 10H_2O$)	10

International Journal of Engineering Research & Technology (IJERT)
ISSN: 2278-0181
Vol. 15 Issue 05 , May - 2026

TABLE III Process parameter for MIG welding

Parameter	Symbol	Optimized value
Arc Voltage	V (V)	210
Welding Speed	S (mm/s)	10
Shielding Gas Flow Rate	Q (L/min)	5
Torch Angle	θ	15°

III. RESULT AND DISCUSSION

The experimental results obtained from the welded AISI 1018 specimens and provides a detailed discussion on the influence of the nanoparticle doped activated flux on weld quality, mechanical performance, and microstructural characteristics. The analysis is based on the four major evaluations conducted during characterization: microstructure examination, macrostructure analysis, micro Vickers hardness measurement, and tensile testing. Each result is interpreted in relation to the welding conditions, flux composition, and heat input behavior. Comparisons are drawn between the flux-coated and no-flux welds wherever applicable (except tensile test, which was conducted only for the coated specimen).

1. Effect of Flux on Weld Bead Geometry

The effect of TiO_2 nanoparticle-doped flux on weld bead geometry was analyzed by comparing the bead characteristics obtained with and without flux coating during MIG welding of AISI 1018 mild steel. The weld bead parameters considered in this study include bead height, bead width, depth of penetration (DOP), internal aspect ratio, and external aspect ratio are summarized in the Table IV.

The experimental results revealed that the application of TiO_2 doped flux improved the overall weld bead characteristics. The bead width increased from 9.6 mm to 10.4 mm, while the depth of penetration improved from 4.2 mm to 4.53 mm, indicating enhanced heat concentration and better fusion characteristics. The internal aspect ratio increased slightly from 0.43 to 0.44, and the external aspect ratio increased from 5.05 to 5.47, indicating the formation of a wider and flatter weld profile. These improvements are attributed to the arc constriction effect and controlled molten metal flow caused by the TiO_2 nanoparticles present in the activated flux. Hence, the TiO_2 doped flux demonstrated superior weld bead geometry and improved welding performance compared to the conventional welding condition without flux.

Overall, the results demonstrate that TiO_2-doped flux plays a significant role in controlling weld geometry by increasing penetration depth and improving the depth-to-width ratio. These improvements are mainly due to enhanced arc constriction and modified weld pool convection, confirming that flux-assisted MIG welding is an effective approach for achieving superior weld penetration and optimized weld morphology.

TABLE IV Effect of TiO_2 Doped Flux on Weld Bead Geometry

S.no	Flux	Bead Height (mm)	Bead Width (mm)	DOP (mm)	Internal Aspect ratio	External Aspect ratio
1	W/o flux	1.9	9.6	4.2	0.43	5.05
2	Tio2 doped flux	1.9	10.4	4.53	0.44	5.47

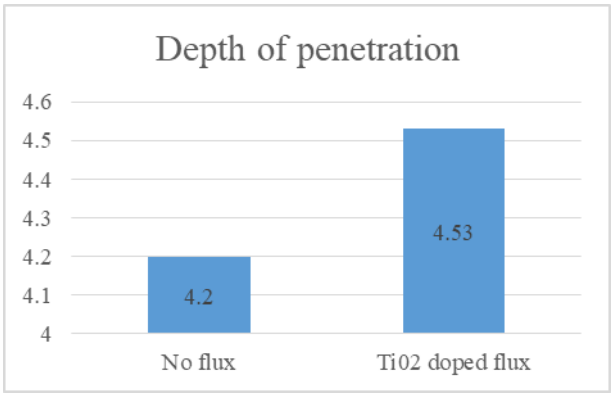

Fig. 1. Effect of flux material on DOP

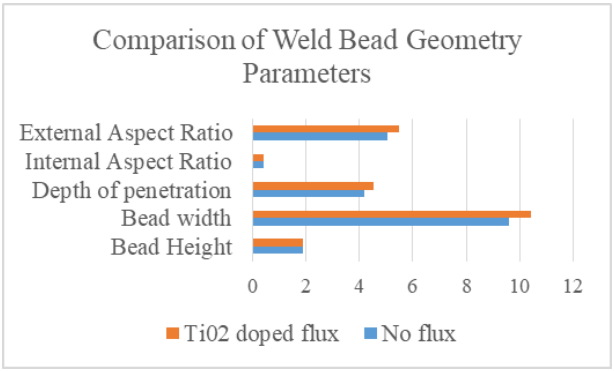

Fig. 2. Comparison of Weld Bead Geometry Parameters

2. Microstructural Analysis

Microstructural examination was carried out to understand the metallurgical changes occurring in the weld metal (WM), heat-affected zone (HAZ), and base metal (BM) due to welding with and without the nanoparticle-doped activated flux. The specimens were ground, polished, and etched using 2% Nital, after which micrographs were obtained at different magnifications. These microstructural images helped in evaluating grain morphology, fusion characteristics, and thermal effects across the weld joint. The observations are discussed for both flux-coated and no-flux welded samples to identify the influence of TiO_2, borax, and extracted electrode flux. The weld metal region of the flux-coated specimen

International Journal of Engineering Research & Technology (IJERT)
ISSN: 2278-0181
Vol. 15 Issue 05 , May - 2026

exhibited a fine dendritic and more compact grain structure, indicating improved solidification behavior.

The presence of TiO_2 nanoparticles in the activated flux enhanced arc constriction, resulting in deeper heat penetration and rapid cooling near the fusion boundary. This promoted the formation of refined dendrites and reduced grain coarsening. The fusion line appeared smooth and well-defined, confirming proper melting and mixing of the base metal. The HAZ showed moderately refined grains compared to the uncoated sample, reflecting controlled heat flow and reduced thermal degradation due to the insulating nature of the flux layer.

In contrast, the no-flux welded sample revealed a coarser and less uniform dendritic structure in the weld metal. The absence of flux contributed to a broader arc and reduced heat concentration, causing slower cooling rates and enlarged grains. The HAZ was noticeably wider, with regions showing grain growth and partial recrystallization. The fusion line in this specimen appeared less distinct, suggesting weaker thermal mixing and less effective heat transfer. The no-flux welded sample shows a coarse and non-uniform grain structure in the fusion zone, indicating weaker arc constriction and lower heat concentration. The wider grain morphology suggests outward Marangoni flow, resulting in shallow penetration and reduced weld pool and the resulting microstructure images of fine grain is shown below.

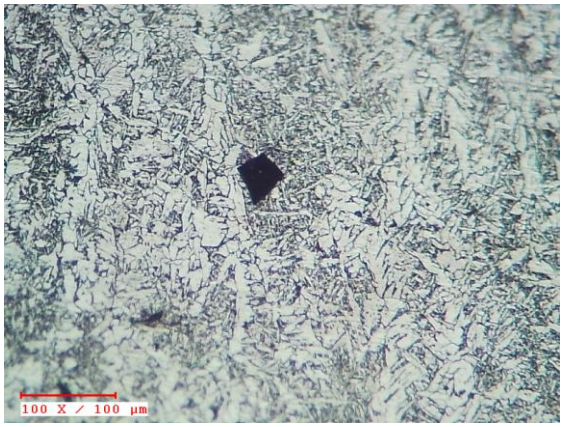

Fig. 3. Weld Zone Microstructure of Flux-Coated Workpiece

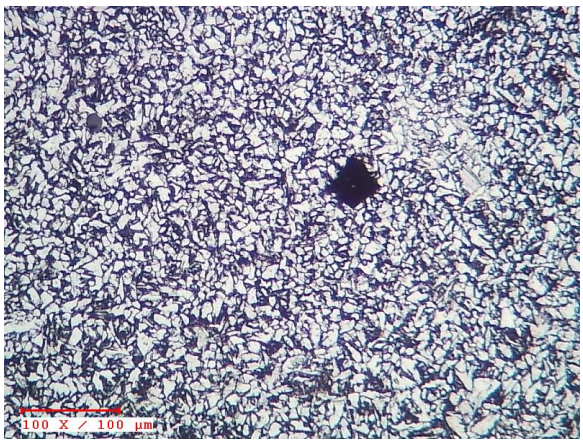

Fig. 4. Weld Zone Microstructure of Non-Flux-Coated Workpiece

3. MACROSTRUCTURE AND BEAD GEOMETRY

Macrostructural evaluation was performed on the welded specimens to study the overall weld bead profile, penetration depth, and fusion behavior. After sectioning, polishing, and etching the samples with 2% Nital, the macro images were captured to clearly reveal the weld boundaries. These images are presented below for comparison in fig 5 & 6.

The macrostructure of the flux-coated specimen displayed a deep and narrow weld bead, indicating strong arc constriction and enhanced downward heat flow. The fusion zone was well defined, with the molten metal penetrating closer to the root, confirming the effect of TiO_2-based activated flux in intensifying heat input. The bead reinforcement on the top surface appeared smooth and uniform, showing that the flux contributed to stable arc behavior during welding. The shape of the weld clearly suggests the presence of reverse Marangoni convection, where molten metal circulates inward toward the weld center, resulting in deeper penetration and a higher depth-to-width ratio.

In contrast, the no-flux specimen exhibited a wider and shallower bead profile. The fusion line was less concentrated, and the penetration depth was noticeably lower compared to the flux-coated sample.

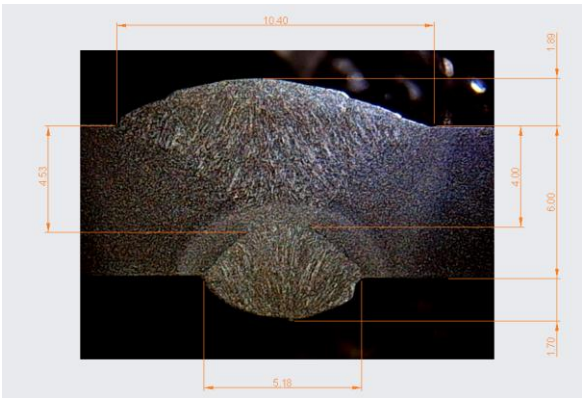

Fig. 5. Macrostructure of flux coated workpiece

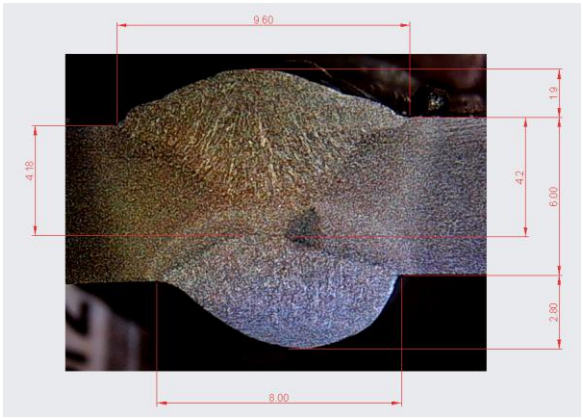

Fig. 5. Macrostructure of without flux

International Journal of Engineering Research & Technology (IJERT)
ISSN: 2278-0181
Vol. 15 Issue 05 , May - 2026

4. Micro Vickers Hardness Distribution

The hardness values indicate that the no-flux sample consistently exhibits slightly higher hardness across the weld metal, HAZ, and base metal compared to the flux coated sample. In the weld metal, this marginal increase (188 HV vs. 186 HV) suggest a slightly faster cooling rate without flux, leading to finer microstructural features. The HAZ of the no-flux joint also shows higher hardness (187 HV), likely due to greater thermal exposure and grain refinement caused by outward Marangoni flow. The base metal hardness difference (224 HV vs. 215 HV) reflects natural material variation and minor thermal influence during welding. Overall, the flux-coated weld produces smoother bead shape and deeper penetration, but the no-flux sample shows slightly higher hardness because of higher cooling rates and less arc constriction which is shown in Table V.

TABLE V Micro Vickers Hardness Values of Welded Specimens

Location	Flux Coated Sample (HV)	No Flux Sample (HV)
Weld metal (WM)	186	188
Heat-Affected Zone (HAZ)	181	187
Base Metal	215	224

5. TENSILE TEST RESULTS

Tensile testing was carried out on the flux-coated weld specimen to evaluate the mechanical performance of the welded joint under uniaxial loading. The sample was prepared in a standard dumbbell (dog-bone) profile according to ASTM E8/E8M specifications, ensuring uniform gauge length and accurate load distribution during testing. The welded region was positioned centrally in the gauge section so that the applied tensile load would directly assess the strength of the weld metal and adjacent heat-affected zone. The test was performed using a calibrated Universal Testing Machine (UTM), where the specimen was subjected to a gradually increasing tensile load until fracture occurred.

TABLE VI Tensile Test Results for Flux-Coated Welded Specimen

Parameter	Result
Ultimate Tensile Strength (MPa)	662
Fracture location	HAZ (Ductile)

The fracture location observed on the tested specimen provides additional insight. In most welded joints, failure tends to occur either in the heat-affected zone or in a weaker section of the weld metal. The location recorded in Table VI helps identify whether the flux contributed to strengthening the weld region. If the failure occurred away from the weld—typically in the base metal—it suggests that the weld metal was stronger than the parent material, indicating excellent weld integrity.

IV. CONCLUSION

This study investigated the influence of a specially formulated nanoparticle-doped activated flux on the MIG welding performance of AISI 1018 mild steel. The flux mixture, consisting of TiO_2 nanoparticles, borax, and extracted electrode flux blended with an acetone–isopropanol solvent, significantly enhanced the welding characteristics. The microstructural analysis showed that the flux-coated weld exhibited finer and more compact dendritic grains due to improved arc constriction and controlled heat flow. Macrostructural observations confirmed deeper penetration and a sharper fusion boundary, indicating effective modification of molten metal flow. The hardness distribution across the weldment displayed higher and more consistent values in the flux-coated sample, reflecting refined microstructure and efficient thermal regulation. The tensile test further validated the weld strength. Overall, the results confirm that the activated flux contributed to improved weld quality, enhanced penetration, and better mechanical performance compared to conventional MIG welding without flux.

REFERANCES

[1] A. Baghel, C. Sharma, S. Rathee, and M. Srivastava, “Influence of activated flux on micro-structural and mechanical properties of AISI 1018 during MIG welding,” *Materials Today: Proceedings*, Elsevier, 2021.

[2] I. A. Ibrahim, S. A. Mohamat, A. Amir, and A. Ghalib, “The effect of Gas Metal Arc Welding (GMAW) processes on different welding parameters,” *Procedia Engineering*, vol. 41, pp. 1502-1506, 2012.

[3] H. P. R. Pydi, A. Pradeep, S. Vijayakumar, and R. Srinivasan, “Examination of various weld process parameters in MIG welding of carbon steel on weld quality using radiography and magnetic particle testing,” *Materials Today: Proceedings*, vol. 62, pp. 1909-1912, 2022.

[4] S. Mahesh and V. Appalaraju, “Optimization of MIG welding parameters for improving strength of welded joints,” *International Journal of Innovative Technology and Research*, vol. 5, no. 3, pp. 6453-6458, 2017.

[5] A. P. Sadewo, H. Ardiyannata, and A. Purniawan, “Effect of acetone/isopropanol as solvent TiO_2 active flux on penetration characteristics of activated tungsten inert gas welding of Incoloy 825,” *IOP Conference Series: Materials Science and Engineering*, vol. 546, pp. 1-7, 2019.

[6] G. Senthil Kumar, U. Natarajan, and S. S. Ananthan, “Vision inspection system for the identification and classification of defects in MIG welding joints,” *International Journal of Advanced Manufacturing Technology*, vol. 61, pp. 923-933, 2011.

[7] M. Aghakhani, M. R. Ghaderi, A. Karami, and A. A. Derakhshan, “Combined effect of TiO_2 nanoparticles and input welding parameters on the weld bead penetration in submerged arc welding process using fuzzy logic,” *International Journal of Advanced Manufacturing Technology*, vol. 71, pp. 763-772, 2013.

[8] S. L. Lawal, S. A. Afolalu, T.-C. Jen, and E. T. Akinlabi, “Tungsten inert gas (TIG) and metal inert gas (MIG) welding applications – critical review,” *E3S Web of Conferences*, vol. 390, 05012, 2023.

[9] I. Acar, B. Cevik, and B. Gulenc, “Weldability of dissimilar stainless steels by MIG welding with different gas combinations,” *Sādhanā*, vol. 48, article 69, 2023.

[10] Z. H. Mohsen, A. B. Abdulwahhab, and M. Abbas, “Study effect of

International Journal of Engineering Research & Technology (IJERT)
ISSN: 2278-0181
Vol. 15 Issue 05 , May - 2026

active flux on mechanical properties of TIG welding process," *Results in Engineering*, vol. 26, article 101468, 2025.

[11] S. Acharya and S. Das, "A review on the use of activating flux in gas tungsten arc welding towards obtaining high productivity," *Manufacturing Technology Today*, vol. 22, no. 7-8, pp. 12-18, 2023.

[12] Y. Liu, J. Wang, S. Lin, L. Gu, B. Yan, D. Zhang, L. Xiao, L. Yan, G. Zhu, and X. Zeng, "A dissimilar laser welding joint of magnesium alloys AZ80 and AM60: Microstructure analysis and mechanical behavior," *Journal of Magnesium and Alloys*, article in press, 2025.

[13] G. Dak and C. Pandey, "Study on effect of weld groove geometry on mechanical behavior and residual stresses variation in dissimilar welds of P92/SS304L steel for USC boilers," *Archives of Civil and Mechanical Engineering*, vol. 22, article 140, 2022.